**Supporting Information (SI)**

**For**

**Architectural control of urea in supramolecular 1D strontium vanadium oxide chains**

## 1. Instrumentation

**Elemental analysis:** Euro Vector Euro EA 3000 elemental analyzer.

**Single-crystal X-Ray Diffraction (XRD):** Nonius Kappa CCD single-crystal X-ray diffractometer ($\lambda$(Mo-K$_\alpha$) = 0.71073 Å) equipped with a graphite monochromator.

**UV-Vis spectroscopy:** UV-Vis spectra from 200 to 1000 nm were collected on a Shimadzu UV-2401 PC UV-Vis spectrophotometer in transmission mode using quartz cuvettes with 1.0 cm optical path length. UV-Vis spectra from 200 to 1600 nm were collected on a Shimadzu UV-3600 UV-Vis-NIR spectrophotometer in transmission mode using quartz cuvettes with 1.0 cm optical path length.

**Fourier-transform infrared (FT-IR) spectroscopy:** Unless stated otherwise, the materials were prepared as KBr pellets. FT-IR spectra were collected in transmission mode using a Shimadzu FT-IR-8400S spectrometer. FT-IR spectroscopy of compound **2** was performed on a Shimadzu FT-IRPrestige-21 spectrometer including a Golden Gate ATR-unit. Signals are given in wavenumbers (cm$^{-1}$), intensities are denoted as vs = very strong, s = strong, m = medium, w = weak, b = broad.

**Mass spectrometry:** Electrospray-ionization mass spectrometry (ESI-MS) was performed using *ultra-high resolution* time-of-flight (UHR-TOF) Bruker Daltonik maXis mass spectrometer in negative ion detection mode. Measurement conditions: source voltage: 4 kV, sample flow rate: 500 µl/h, drying gas temperature (N$_2$): 180 °C. Before each series of measurements the spectrometer was calibrated with Agilent "ESI-TOF low concentration tuning mixture".

**General remarks:** All chemicals were purchased from Sigma Aldrich, ABCR or ACROS and were of reagent grade. The chemicals were used without further purification unless stated otherwise.

## 2. Synthetic section

### 2.1. Synthesis of 1: $\{[Sr(dmf)_3(CON_2H_4)_2][Sr(dmf)_2(CON_2H_4)_2][H_2V_{10}O_{28}]\}$

$(^nBu_4N)_3[H_3V_{10}O_{28}]$ (0.20 g, 0.12 mmol), $SrBr_2 \cdot 6\ H_2O$ (0.09 g, 0.25 mmol) and $CON_2H_4$ (0.06 g, 1.07 mmol) were suspended in *N,N*-dimethyl formamide (DMF, 6 ml) and the reaction mixture was heated to 70 °C for 2 h. Thereby the color changed from orange to reddish orange and slight turbidity occurred. After the addition of $H_2O$ (250 µl) the solution turned clear. Diffusion crystallization with acetone as diffusion solvent resulted in yellow crystalline plates. The crude product was washed with acetone and was air-dried.

**Yield:** 10.2 mg (5.87 µmol, 4.89 % based on V)

**Elemental analysis in wt.-% for $Sr_2V_{10}O_{37}C_{19}N_{13}H_{53}$ (calcd.):** C 12.83 (13.11), N 10.26 (10.46), H 2.96 (3.07).

**Characteristic IR-bands (in $cm^{-1}$):** 3325 (m, b), 3210 (m, b), 2933 (w), 1646 (vs), 1624 (vs), 1566 (s), 1495 (s), 1432 (s), 1250 (m), 981 (s), 940 (vs), 826 (vs).


### 2.2. Synthesis of 2: $\{[Sr(dmf)_4]_2[H_2V_{10}O_{28}]\}$

$(^nBu_4N)_3[H_3V_{10}O_{28}]$ (0.409 g, 0.24 mmol) and $SrBr_2 \cdot 6\ H_2O$ (0.173 g, 0.49 mmol) were dissolved in DMF (5 ml). After the addition of $H_2O$ (400 µl) the orange solution was heated to 70 °C for 2 h. Diffusion crystallization with acetone as diffusion solvent yielded single orange crystalline blocks. The crude product was washed with acetone and was air-dried.

**Yield:** 155.1 mg (0.09 mmol, 75 % based on V)

**Elemental analysis in wt.-% for $Sr_2V_{10}O_{36}C_{24}N_8H_{58}$ (calcd.):** C 16.83 (16.77), N 6.08 (6.52), H 3.42 (3.40).

**Characteristic IR-bands (in $cm^{-1}$):** 2934 (w), 2353 (m), 1663 (vs), 1385 (m), 1109 (m), 972 (vs), 837 (s), 755 (m).
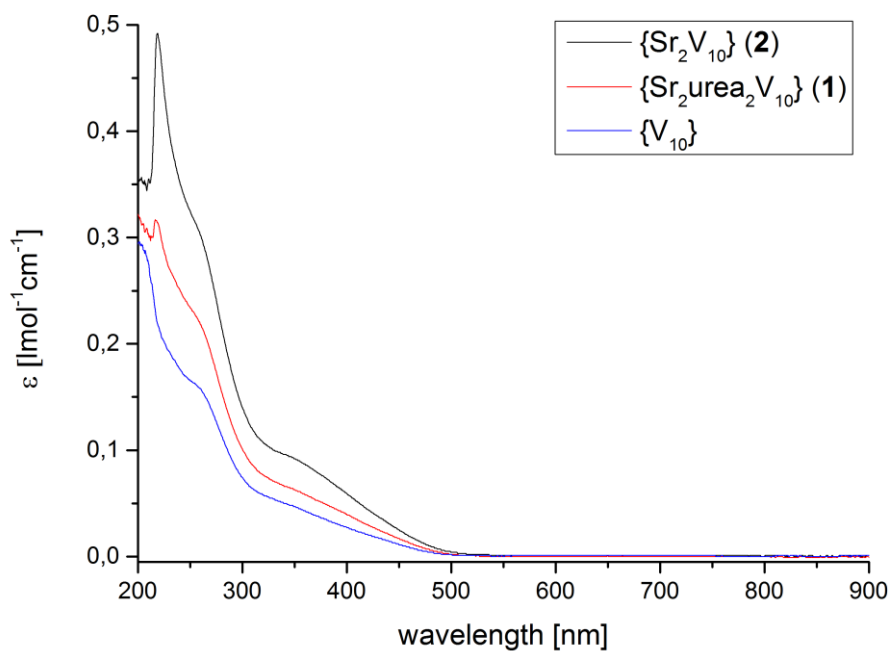
## 3. UV-Vis spectroscopy



**Figure 1:** Room temperature UV-Vis spectra of $\{V_{10}\}$, **1**, **2** recorded in methanolic solution (c = 2.5 x $10^{-4}$ M).

## 4. Mass spectrometry

### 4.1. $\{[Sr(dmf)_3(CON_2H_4)_2][Sr(dmf)_2(CON_2H_4)_2][V_{10}O_{28}]\}$ (1)

| Found m/z | Simulated m/z | Charge | Assignment |
|-----------|---------------|--------|------------|
| 280.7903 | 280.7918 | 2- | $[V_6O_{16}]^{2-}$ |
| 413.1878 | 413.1899 | 2- | $[V^V_8V^{IV}O_{23}]^{2-}$ |
| 454.6567 | 454.6568 | 2- | $[V^V_8V^{IV}_2O_{25}]^{2-}$ |
| 462.6532 | 462.6543 | 2- | $[V_{10}O_{26}]^{2-}$ |
| 480.6623 | 480.6648 | 2- | $[H_4V_{10}O_{28}]^{2-}$ |

**Table 1:** Cluster units and fragments of compound **1** assigned by analysis of negative-mode ESI-MS spectra.
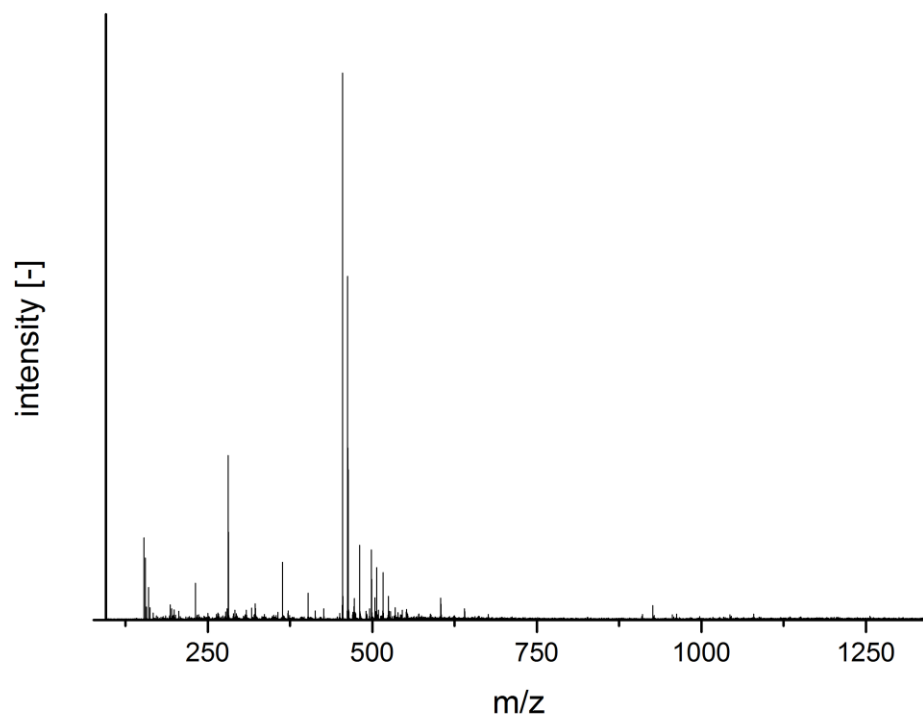
**Figure 2:** Negative-mode high resolution ESI mass spectrum of **1** in DMF (c = 5 x 10$^{-5}$ M).
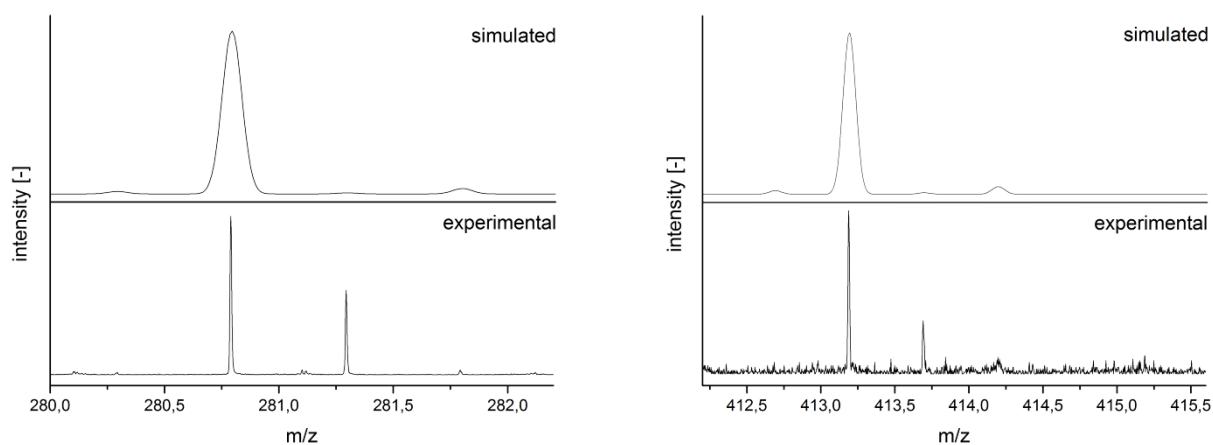


**Figure 3: Left:** Experimental and simulated ESI mass spectrum of $[V_6O_{16}]^{2-}$ observed at m/z = 280.7903. **Right:** Experimental and simulated ESI mass spectrum of $[V^V_8V^{IV}O_{23}]^{2-}$ observed at m/z = 413.1878.
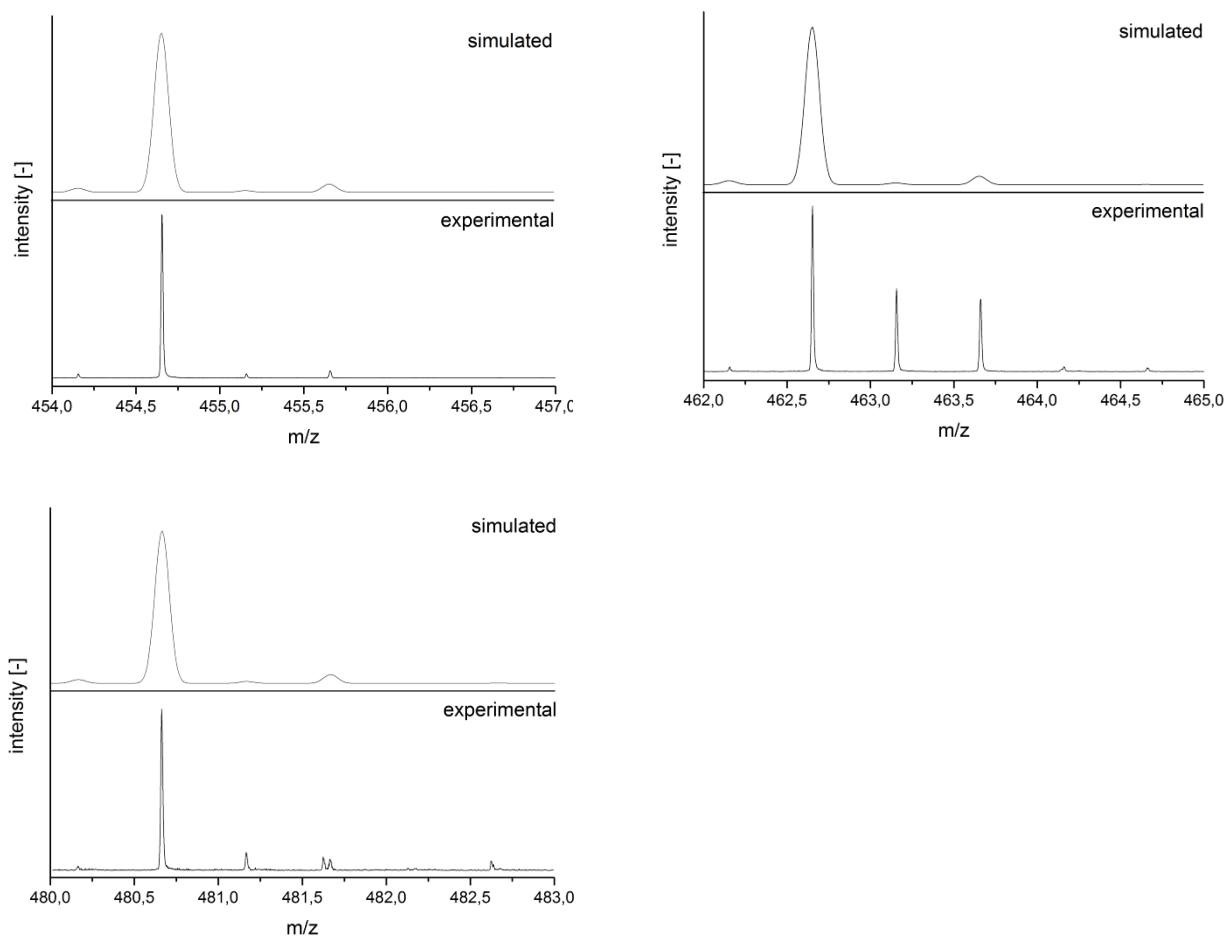
**Figure 4: Top Left:** Experimental and simulated ESI mass spectrum of $[V^V_8V^{IV}_2O_{25}]^{2-}$ observed at m/z = 454.6567. **Top Right:** Experimental and simulated ESI mass spectrum of $[V_{10}O_{26}]^{2-}$ observed at m/z = 462.6532. **Bottom Left:** Experimental and simulated ESI mass spectrum of the principal building block $[H_4V_{10}O_{28}]^{2-}$ observed at m/z = 480.6623.

## 4.2.   {[Sr(dmf)$_4$]$_2$[V$_{10}$O$_{28}$]} (2)

| Found m/z | Simulated m/z | Charge | Assignment |
|:---:|:---:|:---:|:---:|
| 280.7917 | 280.7918 | 2- | $[V_6O_{16}]^{2-}$ |
| 330.7603 | 330.7600 | 2- | $\{H[V_7O_{19}]\}^{2-}$ |
| 371.7229 | 371.7230 | 2- | $[V_8O_{21}]^{2-}$ |
| 380.7277 | 380.7283 | 1- | $\{H[V_4O_{11}]\}^{-}$ |
| 423.6718 | 423.6733 | 2- | $[SrV_8O_{22}]^{2-}$ |
| 462.6529 | 462.6543 | 2- | $[V_{10}O_{26}]^{2-}$ |
| 480.6630 | 480.6648 | 2- | $\{H_4[V_{10}O_{28}]\}^{2-}$ |
| 514.6045 | 514.6046 | 2- | $[SrV_{10}O_{27}]^{2-}$ |
| 519.1053 | 519.1072 | 4- | $\{H_2[SrV_{10}O_{28}][SrV_{10}O_{27}]\}^{4-}$ |
| 531.9197 | 531.9213 | 3- | $\{[SrV_{10}O_{28}][SrV_5O_{13}]\}^{3-}$ |
| 540.5796 | 540.5798 | 4- | $\{[Sr_2V_{10}O_{28}][SrV_{10}O_{27}]\}^{4-}$ |
| 686.4734 | 686.4752 | 3- | $\{H[SrV_{10}O_{28}][SrV_{10}O_{26}]\}^{3-}$ |

| | | | |
|---|---|---|---|
| 692.4791 | 692.4787 | 3- | $\{H_3[SrV_{10}O_{28}][SrV_{10}O_{27}]\}^{3-}$ |
| 721.1093 | 721.1088 | 3- | $\{H[Sr_2V_{10}O_{28}][SrV_{10}O_{27}]\}^{3-}$ |
| 748.4152 | 748.4174 | 2- | $\{[SrV_{10}O_{28}][SrV_4O_{10}]\}^{2-}$ |
| 793.8828 | 793.8831 | 4- | $\{[SrV_{10}O_{26}][Sr_2V_{10}O_{28}][SrV_{10}O_{27}]\}^{4-}$ |
| 798.3834 | 798.3858 | 4- | $\{H_2[SrV_{10}O_{27}][Sr_2V_{10}O_{28}][SrV_{10}O_{27}]\}^{4-}$ |
| 802.8888 | 802.8884 | 4- | $\{H_4[SrV_{10}O_{28}][Sr_2V_{10}O_{28}][SrV_{10}O_{27}]\}^{4-}$ |
| 807.3891 | 807.3910 | 4- | $\{H_6[V_{10}O_{28}][Sr_2V_{10}O_{28}][Sr_2V_{10}O_{28}]\}^{4-}$ |
| 819.8577 | 819.8583 | 4- | $\{[SrV_{10}O_{26}][Sr_2V_{10}O_{28}][Sr_2V_{10}O_{28}]\}^{4-}$ |
| 824.3614 | 824.3609 | 4- | $\{H_2[SrV_{10}O_{27}][Sr_2V_{10}O_{28}][Sr_2V_{10}O_{28}]\}^{4-}$ |
| 876.9840 | 876.9840 | 3- | $\{H[SrV_4O_{11}][Sr_2V_{10}O_{28}][SrV_{10}O_{27}]\}^{3-}$ |

**Table 2:** Cluster fragments and poly-cluster assemblies of compound **2** assigned by analysis of negative-mode ESI-MS spectra.
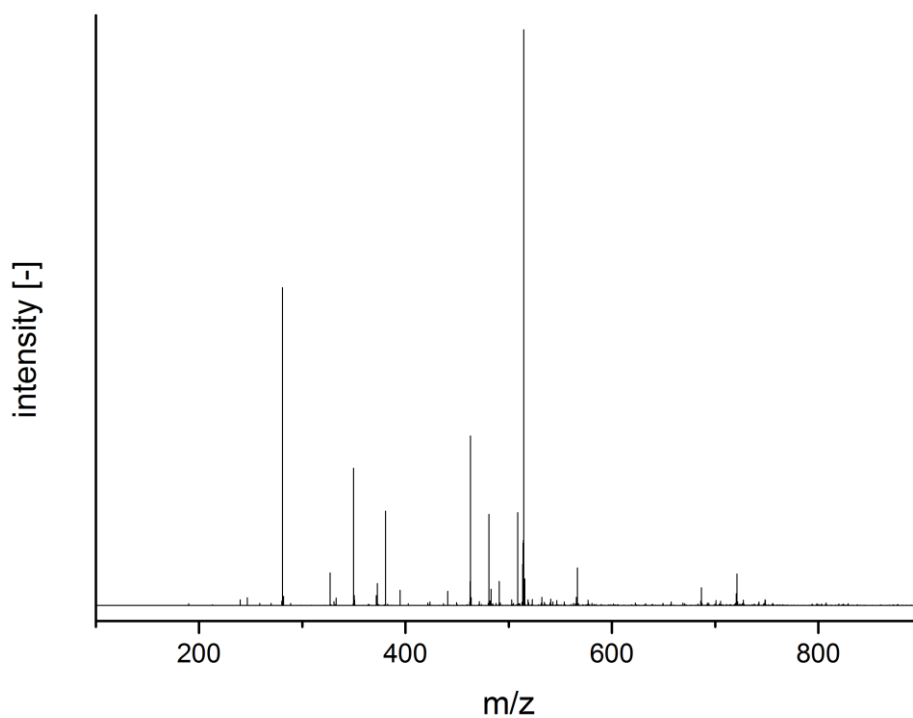


**Figure 5:** Negative-mode high resolution ESI mass spectrum of **2** in methanol (c = 5 x $10^{-5}$ M).
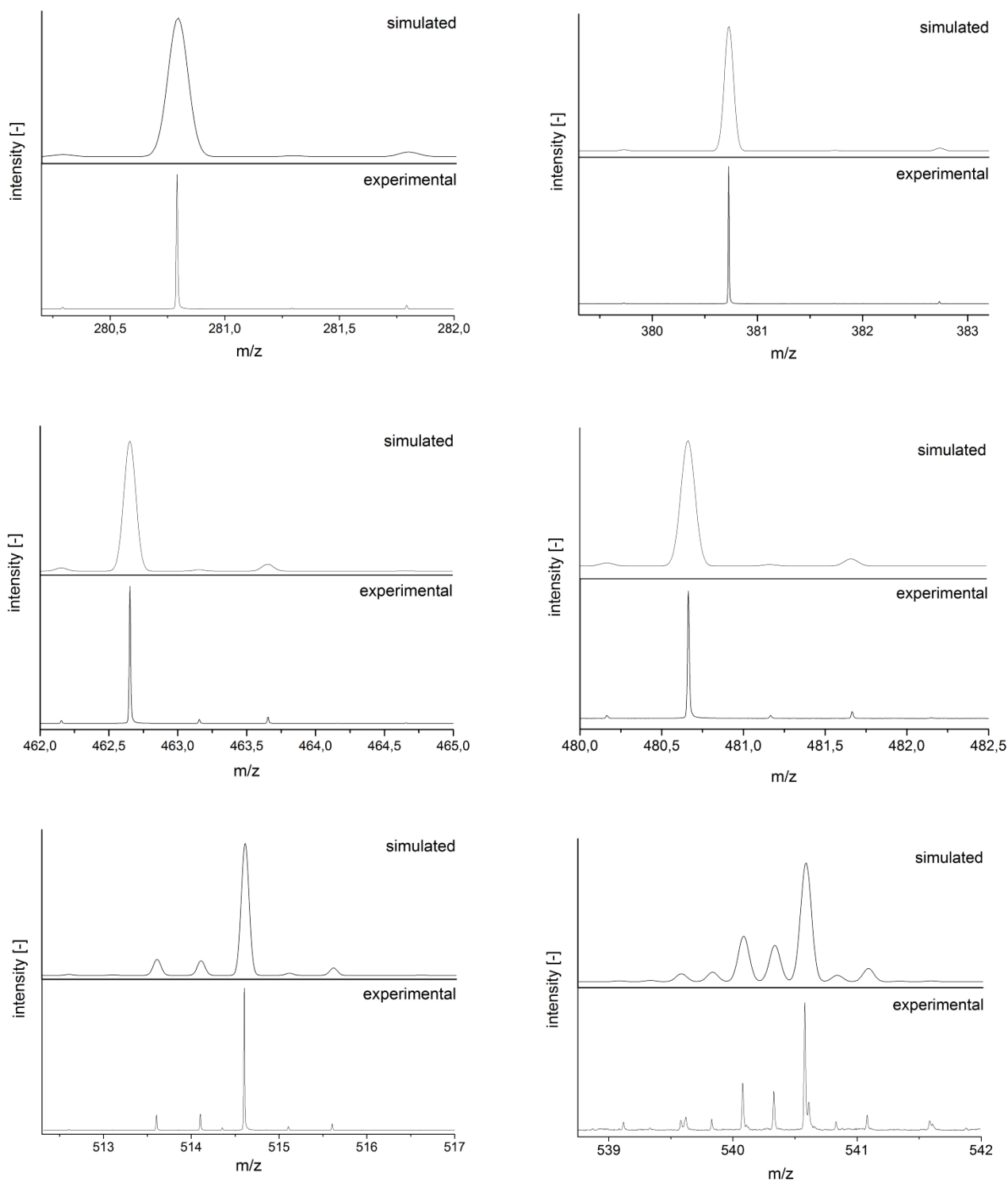
**Figure 6: Top Left:** Experimental and simulated ESI mass spectrum of $[V_6O_{16}]^{2-}$ observed at m/z = 280.7917.
**Top Right:** Experimental and simulated ESI mass spectrum of $\{H[V_4O_{11}]\}^-$ observed at m/z = 380.7277.
**Middle Left:** Experimental and simulated ESI mass spectrum of $[V_{10}O_{26}]^{2-}$ observed at m/z = 462.6529.
**Middle Right:** Experimental and simulated ESI mass spectrum of $\{H_4[V_{10}O_{28}]\}^{2-}$ observed at m/z = 480.6630.
**Bottom Left:** Experimental and simulated ESI mass spectrum of $[SrV_{10}O_{27}]^{2-}$ observed at m/z = 514.6045.
**Bottom Right:** Experimental and simulated ESI mass spectrum of $\{[Sr_2V_{10}O_{28}][SrV_{10}O_{27}]\}^{4-}$ observed at m/z = 540.5796.
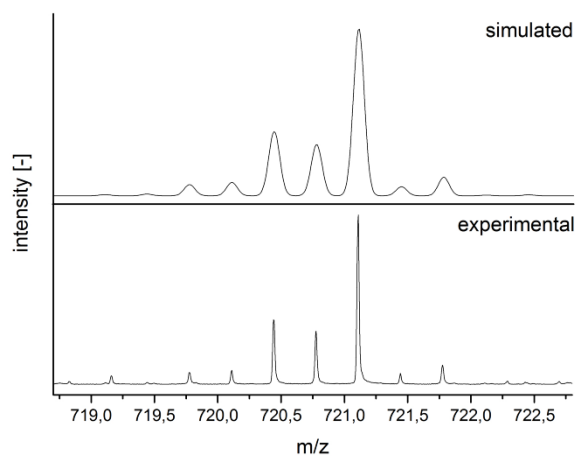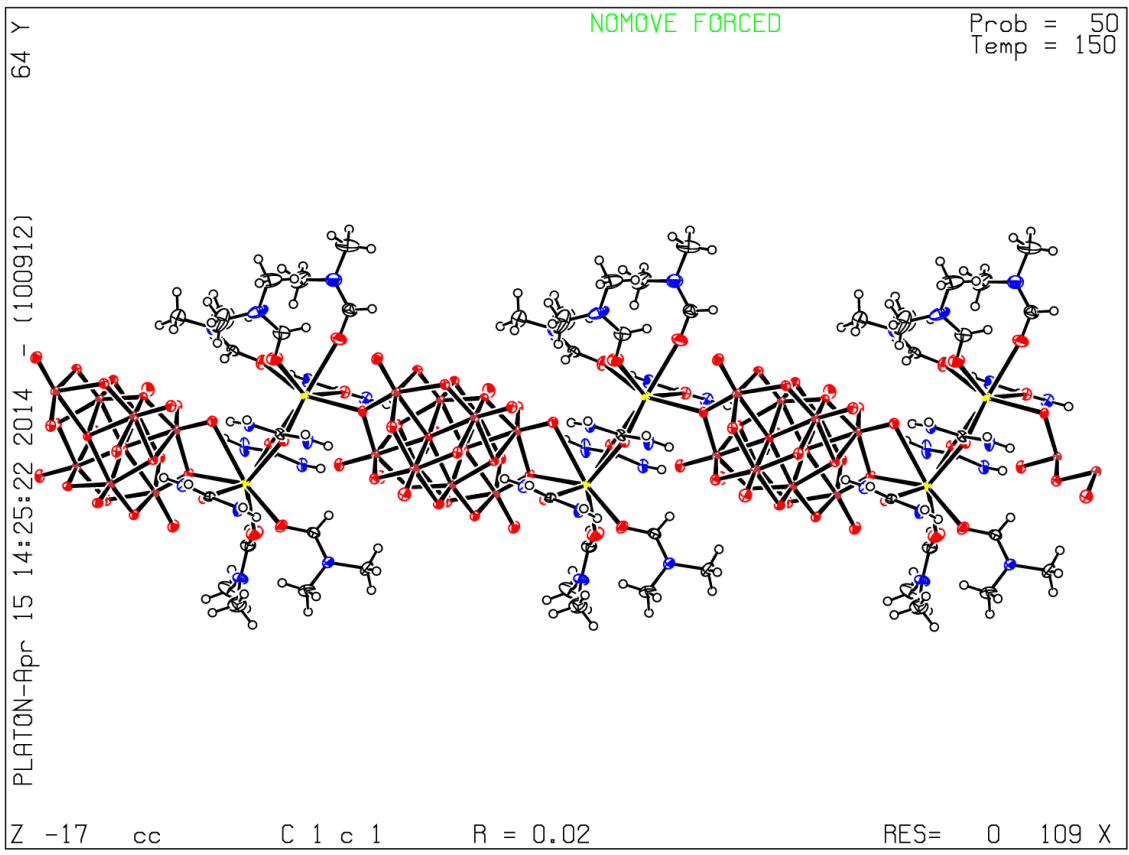
**Figure 7:** Experimental and simulated ESI mass spectrum of $\{H[Sr_2V_{10}O_{28}][SrV_{10}O_{27}]\}^{3-}$ observed at m/z = 721.1093.

## 5. Crystallographic Section

### 5.1. {[Sr(dmf)$_3$(CON$_2$H$_4$)$_2$][Sr(dmf)$_2$(CON$_2$H$_4$)$_2$][H$_2$V$_{10}$O$_{28}$]} (1)

| | |
|---|---|
| CCDC code | 1027675 |
| Empirical formula | $C_{19}H_{53}N_{13}O_{37}Sr_2V_{10}$ |
| Formula weight | 1740.36 |
| Temperature/K | 150.15 |
| Crystal system | monoclinic |
| Space group | Cc |
| a/Å | 10.8044(5) |
| b/Å | 23.2995(14) |
| c/Å | 22.2340(11) |
| α/° | 90 |
| β/° | 100.681(4) |
| γ/° | 90 |
| Volume/Å$^3$ | 5500.1(5) |
| Z | 4 |
| $\rho_{calc}$g/cm$^3$ | 2.099 |
| μ/mm$^{-1}$ | 3.644 |
| F(000) | 3432.0 |
| Crystal size/mm$^3$ | 0.25 × 0.2 × 0.15 |
| Radiation | MoKα ($\lambda$ = 0.71073) |
| 2Θ range for data collection/° | 12.47 to 53.002 |
| Index ranges | -13 ≤ h ≤ 13, -29 ≤ k ≤ 29, -27 ≤ l ≤ 27 |
| Reflections collected | 38057 |
| Independent reflections | 10852 [R$_{int}$ = 0.0227, R$_{sigma}$ = 0.0259] |
| Data/restraints/parameters | 10852/652/741 |
| Goodness-of-fit on F$^2$ | 1.054 |
| Final R indexes [I>=2σ (I)] | R$_1$ = 0.0198, wR$_2$ = 0.0458 |
| Final R indexes [all data] | R$_1$ = 0.0229, wR$_2$ = 0.0467 |
| Largest diff. peak/hole / e Å$^{-3}$ | 0.69/-0.38 |
| Flack parameter | -0.0033(16) |

NOMOVE FORCED

Prob =   50
Temp = 150

PLATON-Apr 15 14:25:22 2014   -  (100912)

Z  -17    cc        C 1 c 1      R = 0.02                    RES=    0   109 X

## 5.2. {[Sr(dmf)₄]₂[H₂V₁₀O₂₈]} (2)

| | |
|---|---|
| CCDC code | 1027674 |
| Empirical formula | $C_{24}H_{58}N_8O_{36}Sr2V_{10}$ |
| Formula weight | 17191.4 |
| Temperature/K | 150 |
| Crystal system | triclinic |
| Space group | P-1 |
| a/Å | 10.9593(3) |
| b/Å | 11.6409(7) |
| c/Å | 12.2782(7) |
| α/° | 104.697(4) |
| β/° | 99.497(4) |
| γ/° | 109.603(3) |
| Volume/Å³ | 1372.51(13) |
| Z | 2 |
| $\rho_{calc}g/cm^3$ | 2.078 |
| $\mu/mm^{-1}$ | 3.646 |
| Crystal size/mm³ | $0.25 \times 0.2 \times 0.15$ |
| Radiation | MoKα (λ = 0.71073) |
| 2Θ range for data collection/° | 12.438 to 53 |
| Index ranges | $-13 \leq h \leq 13, -14 \leq k \leq 14, -15 \leq l \leq 15$ |
| Reflections collected | 34533 |
| Independent reflections | 5609 [$R_{int}$ = 0.0232, $R_{sigma}$ = 0.0150] |
| Data/restraints/parameters | 5609/562/398 |
| Goodness-of-fit on F² | 1.047 |
| Final R indexes [I>=2σ (I)] | $R_1$ = 0.0280, $wR_2$ = 0.0699 |
| Final R indexes [all data] | $R_1$ = 0.0342, $wR_2$ = 0.0747 |
| Largest diff. peak/hole / e Å⁻³ | 1.31/-1.07 |